SCIENCE CHINA
Technological Sciences

Special Topic: Nuclear Science and Technology
• Article •

January 2014 Vol.57 No.1: 14–18
doi: 10.1007/s11431-013-5413-0

Optimization and temperature effects on sandwich betavoltaic microbattery

LIU YunPeng, TANG XiaoBin*, XU ZhiHeng, HONG Liang, WANG Peng & CHEN Da

Department of Nuclear Science and Engineering, Nanjing University of Aeronautics and Astronautics, Nanjing 210016, China

Received August 7, 2013; accepted September 11, 2013; published online November 12, 2013

The design scheme of a sandwich-structure betavoltaic microbattery based on silicon using ^{63}Ni is presented in this paper. This structure differs from a monolayer energy conversion unit. The optimization of various physical parameters and the effects of temperature on the microbattery were studied through MCNP. For the proposed optimization design, P-type silicon was used as the substrate for the betavoltaic microbattery. Based on the proposed theory, a sandwich microbattery with a shallow junction was fabricated. The temperature dependence of the device was also measured. The open-circuit voltaic (V_{oc}) temperature dependence of the optimized sandwich betavoltaic microbattery was linear. However, the V_{oc} of the betavoltaic microbattery with a high-resistance substrate exponentially decreased over the range of room temperature in the experiment and simulation. In addition, the sandwich betavoltaic microbattery offered higher power than the monolayer betavoltaic one. The results of this paper provide a significant technical reference for optimizing the design and studying temperature effects on betavoltaics of the same type.

sandwich betavoltaic microbattery, temperature effects, optimization

Citation: Liu Y P, Tang X B, Xu Z H, et al. Optimization and temperature effects on sandwich betavoltaic microbattery. Sci China Tech Sci, 2014, 57: 14–18, doi: 10.1007/s11431-013-5413-0

1 Introduction

The development of microbattery technology has significantly lagged behind that of micro-electromechanical systems (MEMS) and has become a bottleneck in MEMS applications. Several reported microbatteries, such as solar cells and micro fuel cells, do not satisfy the demands of MEMS devices because of their restrictions particularly in terms of service lifetime and energy density. The betavoltaic microbattery, which has a long lifetime and high energy density, has led one of the most important research directions regarding the microbattery and has great potential as a power supply for MEMS.

Many studies have investigated betavoltaics. For example, Qiao et al. [1]. fabricated a ^{63}Ni-Si PIN betavoltaic with 2.45% efficiency, and Pfann et al. [2]. developed a ^{147}Pm-Si betavoltaic with 2.1% efficiency. However, the conversion efficiency of practical Si betavoltaics is much lower than the predicted 14% [3] because of several reasons. First, the energy conversion unit (ECU) employed by the researchers uses only a monolayer structure. Second, various performance parameters of microbatteries, including the thickness of the semiconductor and isotope source, junction depth, doping concentration, and the generation and collection of electron-hole pairs (EHPs), were not optimized. The third reason is the limitations of fabrication technology for semiconductor devices and limitations of the loading methods of radioisotope sources.

In this paper, we present a sandwich-structure ^{63}Ni-Si betavoltaic microbattery. The optimization of physical parameters of the microbattery through different substrates

*Corresponding author (email: tangxiaobin@nuaa.edu.cn)

was discussed in detail by MCNP. A sandwich-structure microbattery with a shallow junction was fabricated. Temperature is one important factor that affects the electrical performance of betavoltaic microbatteries in remote and even hostile environmental conditions, especially in space sensing. Previous study indicated that the temperature dependence of open-circuit voltaics (V_{oc}) was linear for Si PN junction betavoltaics [4]. However, this observation is inapplicable in several conditions. Therefore, temperature effects on betavoltaics are studied in this paper through experiment and simulation.

2 Materials and methods

2.1 Selection of materials

A betavoltaic microbattery is composed of a beta source and a semiconductor junction device. Detailed discussions on selecting beta sources and junction devices are available elsewhere [3]. The selection of beta sources have four important aspects: half-lifetime, energy density, purity, and the effects of radiation damage on semiconductor devices. On one hand, the optimal fabrication of long-lived microbatteries requires the use of isotopes with long half-lifetime. The half-life of 87.44 d for ^{35}S is too short to deliver enough power for many applications. On the other hand, beta sources with high purity are easily protected. Both ^{147}Pm and ^{85}Kr are accompanied by gamma decay despite high energy density. The other key consideration is the threshold for semiconductor radiation damage. For example, the maximum energy of beta particles emitted from ^{90}Sr-Y is 2.284 MeV, which significantly exceeds the threshold (0.151–0.221 MeV) of Si. Because of the low energy of beta particles, the output power is too low for MEMS in the case of ^{3}H. By contrast, ^{63}Ni emits pure beta particles with moderate energy and long half-lifetime. Therefore, among these potential beta sources, ^{63}Ni was selected as the energy source of the betavoltaic in this study.

Many studies on betavoltaics have used wide-band gap semiconductors, including 4H-SiC [5] and GaN [6, 7], because of their strong radiation hardness, low leakage current, and high conversion efficiency. For example, the efficiency limit of GaN reaches 28% [3, 6]. However, the fabrication of wide-band gap semiconductor materials is technically undeveloped and thus introduces many internal defects to ECUs and impairs microbattery performance. The high preparation cost of wide-band gap semiconductors is another problem. By contrast, high technology has made PN junction devices based on silicon cheap and stable [8]. Therefore, Si was used in this study.

2.2 Calculation model

To improve the output power of microbatteries, the calculation model of the betavoltaic with sandwich structure and bidirectional isotope ^{63}Ni sheet was established through MCNP (Figure 1). The betavoltaic is a square cell with a cross-sectional area of 1 cm^2. For upper and lower Si ECUs, the thickness of each deposition layer is 0.05 μm. Deposition layers are used to record the energy deposited at different depths in the ECU.

First, the relationship between conversion units and the available power of the microbattery was calculated by changing the thickness of radioactive ^{63}Ni and Si conversion units. The thickness of each part was then optimized. Second, various optimization performances of the microbattery were obtained. The specific calculation process is similar to that in [9, 10]. The short-circuit current density (J_{sc}) of the betavoltaic was calculated by collecting EHPs from the energy deposition distribution in each layer of the upper and lower ECUs. Through MATLAB, electrical characteristic parameters, such as maximum power density (P_m) and optimized doping concentrations of the betavoltaic, were obtained according to empirical formulas. Empirical formulas of the minority carrier lifetime and mobility ratio were derived from [11–13]. Finally, temperature effects on the J_{sc} and V_{oc} of the microbattery were analyzed. The temperature (T, K) dependence of the band gap (E_g, eV) and the energy (ε, eV) required to generate an EHPS are empirically represented as follows:

$$E_g(T) = 1.170 - 4.73\times10^{-4}T^2/(T+636), \quad (1)$$

$$\varepsilon(T) = 2.8E_g(T) + 0.5. \quad (2)$$

2.3 Experimental methods

Considering the minority carrier diffusion length in practical silicon is much shorter than the theoretical value, a high-resistance p-type Si substrate with a doping concentration of 1.2×10^{12} cm^{-3} was used in the experiment. Theoretical results suggest that a 0.3 μm shallow junction depth grew by doping 1×10^{19} cm^{-3} arsenic ions onto the front of the P-type substrate. Boron ions (1×10^{19} cm^{-3}) were implanted into the reverse side of the substrate to ensure desired ohm contact. The *I-V* characteristics of junction devices irradiated by bidirectional ^{63}Ni and dark current performances were then measured. The temperature effects of the sandwich betavoltaic microbattery on J_{sc} and V_{oc} were

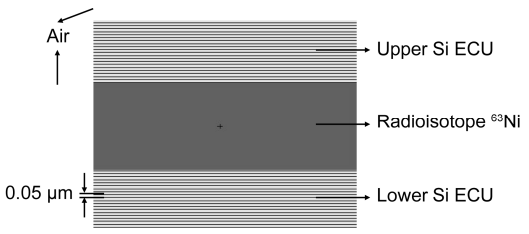

Figure 1 Calculation model of Si betavoltaic microbattery.

also measured, analyzed, and compared with the theoretical results. Simulation initial conditions, including activity of beta source, doped concentrations, and junction depth were the same as those in experiment. The junction area of the ECUs is 0.25 cm^2. For the bidirectional isotope ^{63}Ni sheet used in the experiment, the activity density of one side is 1.85×10^8 Bq/cm^2.

3 Results and discussion

3.1 Thickness design

Available power for the microbattery sharply increased with increasing Si thickness when Si was thin (Figure 2). Available power no longer increased when Si thickness exceeded 20 μm because of two reasons: First, high-energy particles have only a small proportion of the total energy spectrum of ^{63}Ni; second, the maximum range of the beta particles emitted by ^{63}Ni is only 28 μm in silicon. By contrast, when the thickness of the ^{63}Ni sheet was 5 μm, the available power reached its maximum because of the self-absorption of the source and the scattering of silicon. If the thickness increased continuously, the available power nearly remained unchanged, and the self-absorption rate would exceed 0.89.

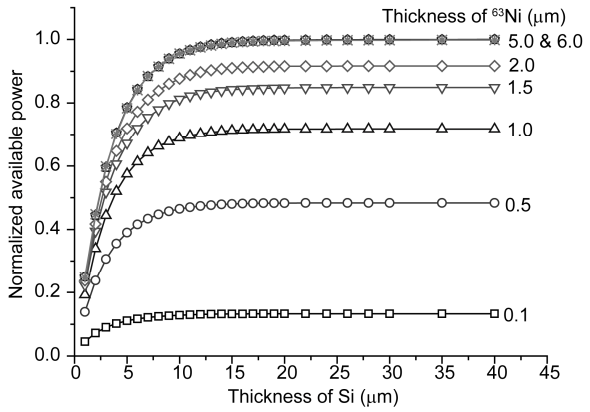

Figure 2 Available power vs. thickness of ^{63}Ni and Si layers.

However, if the thickness of Si is too small, many beta particles will penetrate the junction device and deliver little energy to the microbattery. If the thickness of ^{63}Ni is too small, the activity density of the isotope source will be too low to provide enough power for microbatteries. In addition, when the thickness of ^{63}Ni decreased from 5 μm to 0.5 μm (a 90% decrease), the available power of battery only decreased by approximately 50%, and the self-absorption rate was reduced from 0.89 to 0.43. Therefore, the recommended thicknesses of Si and ^{63}Ni are 10–28 and 0.5–5.0 μm, respectively.

3.2 Performance optimization

Based on the analysis, the thicknesses of ^{63}Ni and Si were set to 2 and 28 μm, respectively, during simulation. Accordingly, the activity density of ^{63}Ni was 3.7×10^9 Bq/cm^2. When the upper and lower ECUs were connected in series, the optimized results of the sandwich betavoltaic microbattery with N-type and P-type substrates were obtained at 300 K by the method mentioned in Section 2.2 (Table 1). The total output performance of the microbattery with a P-type substrate was superior to that with an N-type substrate because the minority carrier diffusion length of P-type Si is greater than that of N-type Si. Most of EHPs are generated in the substrate. High minority diffusion length will increase the collection efficiency of EHPs, and then promote the output power of the microbattery. Although the P^+N junction device has a lower reverse saturation current than the N^+P junction device [9], it prefers the P-type substrate as ECU. A valley was also observed for the efficiency of the microbattery with an N-type substrate at the 0.2 μm junction

Table 1 Optimization parameters of microbatteries with N-type and P-type substrates at different junction depths at 300 K

Optimal parameters	Junction depth (μm)	Optimal N_A (cm^{-3})	Optimal N_D (cm^{-3})	J_{sc} (nA/cm^2)	V_{oc} (V)	P_m (nW/cm^2)	Fill factor	Efficiency (%)
N-type substrate	0.05	4.47×10^{19}	7.94×10^{16}	411.35	0.781	246.12	0.766	7.778
	0.20	8.91×10^{18}	7.94×10^{16}	412.02	0.780	246.07	0.766	7.776
	0.30	6.31×10^{18}	1.12×10^{17}	408.11	0.786	246.10	0.767	7.777
	0.50	3.98×10^{18}	1.12×10^{17}	409.03	0.785	246.26	0.767	7.782
	0.75	2.51×10^{18}	1.26×10^{17}	409.03	0.785	246.50	0.767	7.790
	1.00	$2.00\cdot\times10^{18}$	1.41×10^{17}	408.75	0.786	246.73	0.768	7.797
	2.00	1.00×10^{18}	2.00×10^{17}	409.28	0.787	247.45	0.768	7.820
P-type substrate	0.05	5.62×10^{17}	3.55×10^{19}	417.63	0.812	262.08	0.773	8.282
	0.20	5.62×10^{17}	8.91×10^{18}	417.31	0.810	261.21	0.772	8.255
	0.30	5.62×10^{17}	5.62×10^{18}	417.08	0.809	260.61	0.772	8.236
	0.50	6.31×10^{17}	3.16×10^{18}	415.15	0.809	259.41	0.772	8.198
	0.75	6.31×10^{17}	1.78×10^{18}	414.72	0.806	257.90	0.771	8.150
	1.00	6.31×10^{17}	1.26×10^{18}	413.88	0.804	256.40	0.771	8.103
	2.00	7.08×10^{17}	3.98×10^{17}	411.09	0.794	250.84	0.769	7.927

depth. There was a peek for the reverse saturation current at the 0.2 μm junction depth. For the P-type substrate, the efficiency of the microbattery was monotonically reduced with the increasing junction depth.

3.3 Temperature effects

The temperature dependence of the V_{oc} and J_{sc} of optimized sandwich betavoltaics based on P-type and N-type substrates at the 0.05 μm junction depth is shown in Figure 3. J_{sc} only slightly varied in the range of temperature. Temperature coefficients of J_{sc} of betavoltaics based on P-type and N-type substrates were 0.025% and 0.021%, respectively. This small variation is attributed to the decrease in band gap, and the consequent increase in the number of EHPs. The value of V_{oc} is determined by the ratio of J_{sc} to the reverse saturation current density (J_0) (that is J_{sc}/J_0). The intrinsic carrier concentration exponentially increases with the increase of temperature and the consequent exponential increase in J_0. Then, the ratio J_{sc}/J_0 exponentially decreases with temperature. Therefore, V_{oc} linearly decreased with temperature increase as shown in Figure 3. The sensitivities of the sandwich betavoltaics based on N-type and P-type substrates were −5.87 and −5.75 mV/K respectively.

3.4 Experimental measurements and analysis

Si ECUs were fabricated through the micromachining technology as discussed previously. The upper and lower ECUs were then respectively fixed on the PCB die holders through sheet contact process technology and the consequent down-leads were performed on them (Figure 4(a)). After that, a bidirectional ^{63}N was loaded on the ECU with about 1 mm air gap (Figure 4(b)). In the end, a sandwich betavoltaic was finished by packaging the upper ECU, the lower ECU, and the beta source (Figure 4(c)).

The leakage current densities of the upper and lower ECUs were 0.04 and 0.03 nA/cm^2 at zero bias and 12.65 and 12.31 nA/cm^2 at −10 V bias. These values are slightly high because of two reasons: First, the low doping concentration of the P-type substrate resulted in a high J_0; second,

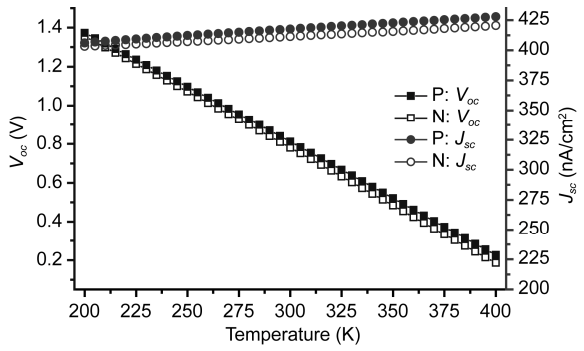

Figure 3 V_{oc} and J_{sc} of betavoltaics with 0.05 μm junction depth and at different temperatures.

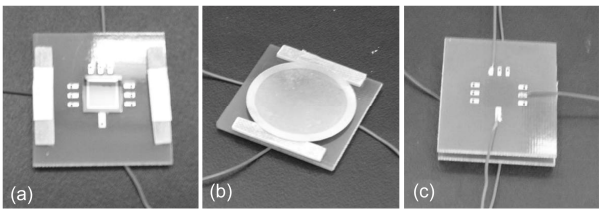

Figure 4 Diagram of the sandwich betavoltaic microbattey: (a) upper or lower ECUs, (b) loading ^{63}Ni, and (c) topview of microbattery.

non-ideality surface treatment, such as passivation, leaded to a high surface leakage current.

Figure 5 shows *I-V* characteristics of the upper and lower ECUs and the sandwich ECUs in series and in parallel irradiated by ^{63}Ni. The maximum output powers of the upper and lower cells were 0.473 and 0.457 nW/cm^2, respectively. In serial connection, the V_{oc} of the sandwich betavoltaic increased, and J_{sc} almost remained unchanged as expected and the consequent maximum output power, which was 0.862 nW/cm^2, increased. In parallel connection, the V_{oc} of the sandwich betavoltaic almost remained unchanged as that of the upper or lower cell, and J_{sc} increased. The consequent maximum output power of the parallel cell was 0.761 nW/cm^2. These results suggest that the sandwich betavoltaic with serial or parallel connections offers a higher power than the monolayer betavoltaic.

The laws of the variation of V_{oc} and J_{sc} with temperature in the experiment were the same as those in the simulation (Figure 6). V_{oc} in the experiment and simulation exponentially decreased over the range of room temperature, in contrast to the results in Figure 3. According to the relationship between V_{oc} and J_{sc}/J_0 [9], when the magnitude of the ratio J_{sc}/J_0 exceeds about 10^3 and increases continually, V_{oc} will arise slightly. In contrast, a little variation in J_{sc}/J_0 will result in a significant change in V_{oc}, when the magnitude of the ratio J_{sc}/J_0 is below about 10^2. The low activity density of the beta sources and high-resistance substrates reduced J_{sc}, increased J_0, and so significantly decreased the consequent ratio J_{sc}/J_0 (which was only 46.39 and 0.05 at 300 K

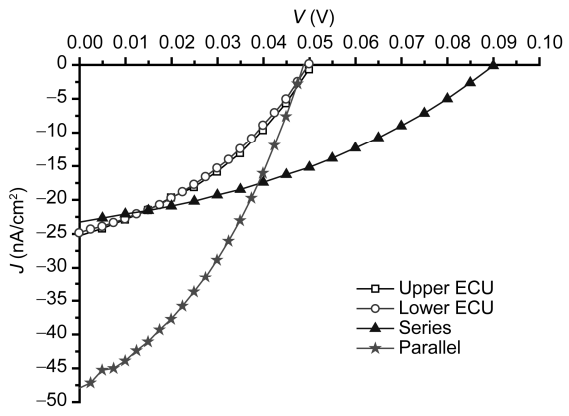

Figure 5 *I-V* curves of betavoltaic batteries with different connection modes.

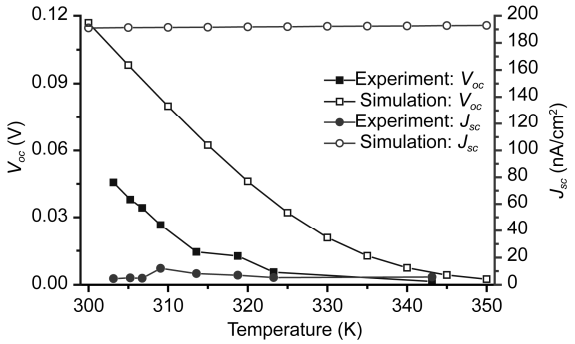

Figure 6 Temperature dependences of V_{oc} and J_{sc} in experiment and simulation.

and 350 K, respectively) that V_{oc} became highly sensitive to temperature. After fitting, the temperature dependence of V_{oc} in the simulation can be expressed by a three-parameter exponential function as follows:

$$V_{oc}(T) = \exp(-84.023 + 0.573T - 9.997T^2). \quad (3)$$

4 Conclusion

A sandwich-structure ^{63}Ni-Si betavoltaic microbattery was studied by simulation and experiment. The output performance of the betavoltaic was optimized at 300 K through MCNP. Based on this method, a sandwich microbattery with a shallow junction was fabricated. The sandwich betavoltaic offered a higher power than the monolayer betavoltaic. For the optimized sandwich betavoltaics, V_{oc} temperature dependence was linear. However, the V_{oc} of betavoltaics with high-resistance substrates exponentially decreased over the range of room temperature in the experiment and simulation. The method presented in this paper can be used to study betavoltaic optimization at different temperatures as well as the temperature effects on betavoltaics with different structural parameters.

This work was supported by the National Natural Science Foundation of China (Grant No. 11205088), the Aeronautical Science Foundation of China (Grant No. 2012ZB52021), the Funding of Jiangsu Innovation Program for Graduate Education (Grant No. CXZZ12_0146), and Fundamental Research Funds for the Central Universities.

1 Qiao D Y, Chen X J, Ren Y, et al. A nuclear micro-battery based on silicon PIN diode. Acta Phys Sin, 2011, 60(2): 155–163
2 Pfann W G, Roosbroeck W V. Radioactive and photoelectric p-n junction power sources. J Appl Phys , 1954, 25(11): 1422–1434
3 Olsen L C. Review of betavoltaic energy conversion. Processing of the 12th Space Photovoltaic Rresearch and Technology Conference. 1993. 256–267
4 Wang G Q, Hu R, Wei H Y, et al. The effect of temperature changes on electrical performance of the betavoltaic cell. Appl Radiat Isotopes, 2010, 68(12): 2214–2217
5 Chandrashekhar M V S, Duggirala R, Spencer M G, et al. 4H-SiC betavoltaic powered temperature transducer. Appl Phys Lett, 2007, 91(5): 053511
6 Tang X B, Liu Y P, Ding D, et al. Optimization design of GaN betavoltaic microbattery. Sci China Tech Sci, 2012, 55(3): 659–664
7 Lu M, Zhang G G, Fu K, et al. Gallium nitride schottky betavoltaic nuclear batteries. Energ Convers Manage, 2011, 52(4): 1955–1958
8 Bao R Q, Brand P J, Chrisey D B. Betavoltaic performance of radiation-hardened high-efficiency Si space solar cells. IEEE T Electron Dev, 2012, 59(5): 1286–1294
9 Tang X B, Ding D, Liu Y P, et al. Optimization design and analysis of Si-^{63}Ni betavoltaic battery. Sci China Tech Sci, 2012, 55(4): 990–996
10 Liu Y P, Tang X B, Ding D, et al. Parameter optimization of GaAs Betavoltaic microbattery. At. Energ Technol, 2012, 46(Sl): 611–616
11 Klaassen D B M. A unified mobility model for device simulation – (I). Model equations and concentration dependence. Solid State Electron, 1992, 35(7): 953–959
12 Klaassen D B M. A unified mobility model for device simulation – (II). Temperature dependence of carrier mobility and lifetime. Solid State Electron, 1992, 35(7): 961–67
13 Reggiani S, Valdinoci M, Colalongo L, et al. An analytical, temperature-dependent model for majority- and minority-carrier mobility in silicon devices. VLSI Des, 2000, 10(4): 467–483